O-311

J. Chem. Thermodynamics **1989**, 21, 351–361

Standard molar Gibbs free energy of formation for Cu_2O: high-resolution electrochemical measurements from 900 to 1300 K

RICHARD D. HOLMES, ANNIE B. KERSTING, and RICHARD J. ARCULUS

Department of Geological Sciences, University of Michigan, 1006 C.C. Little Bldg., Ann Arbor, MI 48109, U.S.A.

(Received 6 October 1988; in final form 20 December 1988)

Oxygen-concentration cells with zirconia solid electrolytes have been used to make equilibrium measurements of the standard molar Gibbs free energy of formation for copper(I) oxide, $\Delta_f G^\circ_m(Cu_2O)$, over the temperature range from 900 to 1300 K. Compared with previous measurements, systematic errors due to thermal gradients across the zirconia solid electrolyte have been greatly reduced. Measurements with three different types of zirconia solid electrolytes have yielded results that differ by only $\pm 40\ J \cdot mol^{-1}$ (± 0.2 mV). This is the best agreement yet achieved between solid electrolytes of different composition. Our recommended value for the standard molar enthalpy of formation, $\Delta_f H^\circ_m(Cu_2O, 298.15\ K)$, is $-(170.59 \pm 0.08)\ kJ \cdot mol^{-1}$ ($p^\circ = 1 \times 10^5$ Pa).

1. Introduction

In our previous study,[1] we showed that oxygen-concentration cells with zirconia solid electrolytes can be used to make exceptionally precise ($\pm 30\ J \cdot mol^{-1}$) measurements of the standard molar Gibbs free energy of formation for transition-metal oxides. The resolution of those experiments was sufficient to show clearly the curvature in $\Delta_f G^\circ_m(T)$, and both the sign and magnitude of the observed curvature closely matched that predicted from the calorimetric values of $\Delta_f C^\circ_{p,m}$. Other evidence, however, led us to conclude that there were small systematic errors ($\approx 0.5\ J \cdot K^{-1} \cdot mol^{-1}$) in the entropy changes $-d\Delta_f G^\circ_m/dT$ of the measured reactions. These errors were apparently due to thermoelectric e.m.f.s produced by temperature gradients across the zirconia solid electrolyte.

Our goals in the present study were to eliminate those systematic errors by reducing the thermal gradients across the solid electrolyte, to eliminate uncertainties in the chemical potential of the reference gas by using pure oxygen instead of air, and to determine whether electrolytes of different composition and configuration could yield identical results.

0021-9614/89/040351+11 $02.00/0

2. Experimental

Figure 1 shows the general features of the experimental apparatus. Compared with our previous apparatus,[1] the most significant changes are the addition of a heat pipe to reduce thermal gradients and the use of pure oxygen as the reference gas.

Three different types of zirconia solid-electrolyte cells were used in our measurements. Two of these were slip-cast sintered tubes supplied by Nippon Kagaku Togyo Co. (Osaka, Japan), having a composition of ($0.89ZrO_2$ + $0.11CaO$) (Type ZR-11) and ($0.92ZrO_2$ + $0.08Y_2O_3$) (Type ZR-8Y). The third type was the "$SIRO_2$ Sensor" supplied by Ceramic Oxide Fabricators Pty. Ltd. (Eagle Hawk, Victoria, Australia), which consists of a small zirconia-electrolyte pellet that is eutectically welded into the end of a long alumina tube. The $SIRO_2$ electrolyte has a composition of 50 mass per cent of ($0.93ZrO_2$ + $0.07Y_2O_3$) mixed with 50 mass per cent of Al_2O_3 in order to reduce the difference in thermal expansion between the electrolyte pellet and the alumina tube.

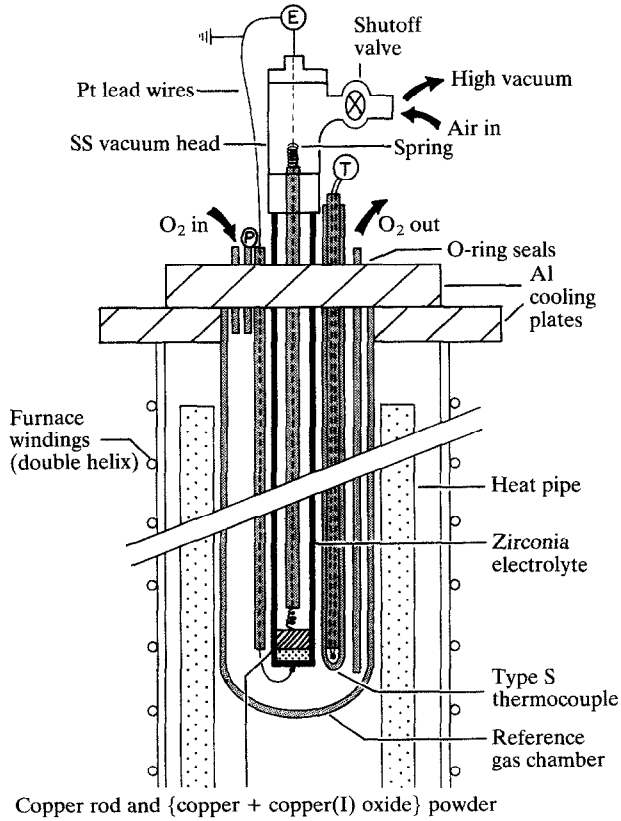

FIGURE 1. Schematic diagram of the solid-electrolyte cell. Zirconia-electrolyte tube: i.d., 5 mm; o.d., 8 mm; length, 300 mm. Reference-chamber tube: i.d., 25 mm; o.d., 32 mm; length, 290 mm. Heat pipe: i.d., 35 mm; o.d., 60 mm; length, 305 mm.

The room-temperature vacuum leak rate of each electrolyte tube was measured at the beginning of the experiment, and sometimes also at its end. Using the rate-of-pressure-rise method, the smallest leak that could be detected with our vacuum system was roughly 10^{-6} Pa·m^3·s^{-1} (of air). The slip-cast ZR-11 and ZR-8Y electrolyte tubes were consistently "leak-free" in these tests, both before and after use at high temperatures. In contrast, all of the $SIRO_2$ electrolyte tubes, except for one, had detectable leaks, typically a factor of 10 to 1000 greater than our limit of detection. These higher leak rates are probably due to the readily observable porosity in the eutectic weld that joins the zirconia pellet to the alumina tube.

Temperature gradients across the zirconia solid-electrolyte cell cause a thermoelectric e.m.f. ($\approx$0.4 mV·K^{-1}) that is indistinguishable from the thermochemical e.m.f. produced by the difference in oxygen pressure between the sample and the reference. Measuring and correcting for these small "thermal residuals" has been a major concern of recent high-accuracy solid-electrolyte experiments.[1,2] This problem has now been overcome by surrounding the high-temperature portion of the cell with a sodium-filled "heat pipe" (Dynatherm Model IFL-11-14-12). The extremely high effective thermal conductivity of the heat pipe[3] reduces thermal gradients within its working volume to insignificant levels and virtually eliminates residual e.m.f.s.

Figure 2(a) shows the residual e.m.f.s measured in our apparatus for the symmetrical cell: Pt|O_2|ZR-11|O_2|Pt. Over the temperature range from 850 to 1300 K, residual e.m.f.s for the ZR-11 electrolytes vary from 0.07 to −0.01 mV with no systematic trend. The average value of (0.02 ± 0.05) mV is equivalent to an error of only 4 J·mol^{-1} in $\Delta_f G^\circ_m(Cu_2O)$. This is more than a factor of 10 smaller than the thermal residuals measured previously.[1,2,4,5] It is so small that no corrections for thermal residuals were deemed necessary for the sample e.m.f.s measured with ZR-11 and ZR-8Y electrolytes.

Residual e.m.f.s for the $SIRO_2$ electrolytes are shown in figure 2(b). They range from 0.08 to −0.23 mV, and the trend appears to change from positive to negative at about 1100 K. In general, these measurements were less stable and less reproducible

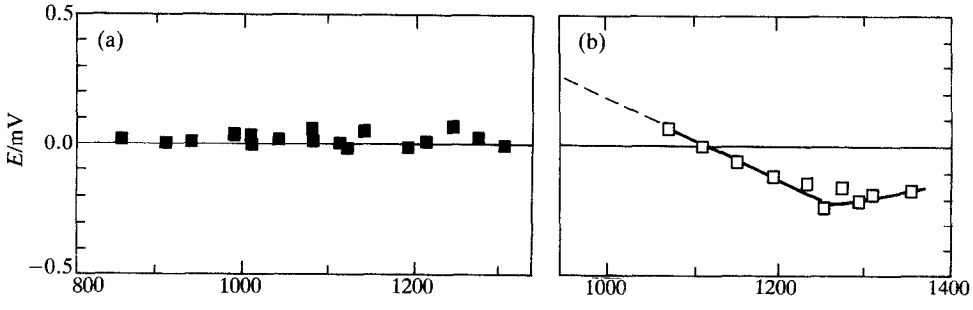

FIGURE 2. Residual e.m.f.s for symmetrical cells. (a): ■, Pt|O_2|ZR-11|O_2|Pt; (b): □, Pt|O_2|$SIRO_2$|O_2|Pt. In both cases, a small slit was cut into the side of the electrolyte tube to ensure that the oxygen pressure at the inner and outer electrodes was identical.

than the ZR-11 residuals. The trend line in figure 2(b) shows the residual corrections that were subtracted from the sample e.m.f.s measured with $SIRO_2$ electrolytes. An uncertainty of perhaps ± 0.2 mV was introduced by the extrapolation of the residual from 1070 to 950 K. This extrapolation was necessary because the {copper + copper(I) oxide} cells with $SIRO_2$ electrolytes gave stable e.m.f.s to temperatures well below the last stable residual.

The reference gas for the measurements reported here was pure oxygen. For high-accuracy measurements, oxygen gas is superior to air for two reasons. First, humidity corrections[2] are unnecessary. Second, systematic errors due to gaseous thermal diffusion in a multi-component mixture[6] are eliminated. The flow rate of oxygen gas through the vacuum-tight reference chamber (100 cm^3) was roughly 0.1 $cm^3 \cdot s^{-1}$. Direct measurements of the gas pressure $p(O_2)$ inside the reference chamber were made with a high-resolution electronic pressure transducer (Setra Systems Model 270, range 80 to 110 kPa, accuracy ± 30 Pa).

Temperatures are based on IPTS-68[7] and were measured with reference-grade Type S thermocouples calibrated against the freezing temperatures of Ag (1235.08 K),[8] and Cu (1358.02 K).[9,10] The purity for both metals (Cominco) was better than 99.9999 mass per cent. The thermocouple calibrations used freezing-temperature cells based on the NBS design[11] and in order to produce identical temperature gradients were carried out in the same furnace used for the e.m.f. measurements. The precision of our routine temperature measurements was ± 0.02 K, and the 12-month drift in the freezing-temperature calibrations was less than 0.1 K. However, the well-known problems caused by inhomogeneities in {platinum + rhodium} thermocouples[12] suggest that ± 0.3 K is a more realistic estimate for the accuracy of these temperature measurements relative to IPTS-68.

Cell and thermocouple e.m.f.s were measured by a digital voltmeter with an NBS-traceable accuracy of ± 0.003 per cent (Solartron Model 7071). The input signals were routed through a computer-controlled switch controller (Fluke Model 2205A). The combined zero offset of the DVM and the switch controller varied from 1 to 2 μV and was corrected to less than 0.1 μV. In runs 2, 4, and 6, a unity-gain "opamp" voltage follower (Analog Devices Model AD545L, $Z > 10^{13}\ \Omega$, $I < 20$ pA) was used as an impedance buffer between the electrochemical cell and the DVM ($Z > 10^{10}\ \Omega$, $I < 20$ pA). There was no measurable difference between the results obtained with and without this impedance buffer.

The wire-wound tube furnace was wrapped in a non-inductive double helix. In order to avoid the interference spikes produced by phase-switched SCRs, a computer-controlled autotransformer was used as the furnace power supply. The e.m.f. circuit was shielded by grounding the heat pipe and by installing a small Inconel cylinder in the gap above the heat pipe. Furnace stability was better than ± 0.15 K.

Two different sample mixtures were used in our measurements. They differed in the initial composition of the oxide phase and in the manufacturer's purity specifications. The "high-purity" sample consisted of {copper + copper(II) oxide} with $m(Cu)/m(CuO) = 8$, where m denotes mass; the purity of both phases was better than 99.999 mass per cent. At high temperatures, the CuO reacted with excess Cu to form the desired sample assemblage of {copper + copper(I) oxide}. The "low-purity"

sample consisted of {copper + copper(I) oxide} with $m(Cu)/m(Cu_2O) = 10$; the purity of Cu was better than 99.9 mass per cent, and the purity of Cu_2O was better than 97 mass per cent. As shown in figure 1, a short length of copper rod was used to compact the loose sample powder; the purity of the Cu rod was better than 99.999 mass per cent. All five materials were obtained from the Aesar Division of Johnson Matthey (Catalog numbers 10609, 10700, 10160, 12300, and 11444). At the beginning of the run, the sample chamber was purged with purified argon (O_2, mass fraction $< 1 \times 10^{-6}$) and then sealed at the high-vacuum shutoff valve.

3. Results

On the basis of the cell reaction:

$$2Cu(s) + \tfrac{1}{2}O_2(g) = Cu_2O(s), \tag{1}$$

the measured values of cell e.m.f., temperature, and reference gas pressure were converted to standard molar Gibbs free energies of formation ($p^\circ = 1 \times 10^5$ Pa) using the relation:

$$\Delta_f G^\circ_m(Cu_2O, T) = -2FE + \tfrac{1}{2}RT \ln\{p(O_2)/p^\circ\}, \tag{2}$$

where $F = 96485.309 \text{ C} \cdot \text{mol}^{-1}$ and $R = 8.314510 \text{ J} \cdot \text{K}^{-1} \cdot \text{mol}^{-1}$.[13] All uncertainties reported here are two standard deviations ($\pm 2s$).

The values of $C^\circ_{p,m}$ and $S^\circ_m(298.15 \text{ K})$ used in the third-law analysis were taken from the JANAF tables.[14] For each of the three phases in reaction (1), the tabulated values of $C^\circ_{p,m}$ were fitted to cubic splines, and the values of $S^\circ_m(T)$ and $H^\circ_m(T)$ at intermediate temperatures were then calculated by integrating the splined $C^\circ_{p,m}$ functions. The calculated values of $\{\Delta_f G^\circ_m(T) - \Delta_f H^\circ_m(298.15 \text{ K})\}$ differ by no more than $4 \text{ J} \cdot \text{mol}^{-1}$ from the heat-capacity functions used in our previous study.[1]

Table 1 gives the results obtained in five runs with the ZR-11 electrolytes. The third-law analysis of these measurements is shown in figure 3(a). (It is uninformative to plot $\Delta_f G^\circ_m$ against T, since the scatter is too small to be seen on this scale, as shown by figure 3 of reference 1.)

Two of the five ZR-11 runs used the "high-purity" {copper + copper(II) oxide} sample, and three runs used the "low-purity" {copper + copper(I) oxide} sample. The figure shows that there was no measurable difference between the two samples. The perfect agreement between these two samples of different starting composition is strong evidence for the attainment of equilibrium by reaction (1). It implies that the conversion reaction:

$$Cu + CuO = Cu_2O, \tag{3}$$

was rapid and effective. Additional evidence for equilibrium is provided by the lack of hysteresis between heating and cooling cycles (figure 3c) and by the immediate stabilization of cell e.m.f. at each new temperature.

Least-squares analysis of the ZR-11 results gave a correlation coefficient of 0.9999989 for a 3-term equation of the form:

$$\Delta_f G^\circ_m/(\text{J} \cdot \text{mol}^{-1}) = a + b(T/\text{K}) + c(T/\text{K})\ln(T/\text{K}), \tag{4}$$

TABLE 1. Experimental results for the cell Pt|(Cu+Cu_2O)|ZR-11|O_2 ($p^\circ = 1 \times 10^5$ Pa)|Pt [a]

T/K	$\Delta_f G^\circ_m(T)$/kJ·mol^{-1}	$\Delta_f H^\circ_m$(298.15 K)/kJ·mol^{-1}	T/K	$\Delta_f G^\circ_m(T)$/kJ·mol^{-1}	$\Delta_f H^\circ_m$(298.15 K)/kJ·mol^{-1}
	Run 2		1150.30	−84.666	−170.633
1159.91	−83.986	−170.637	1191.19	−81.770	−170.644
1210.83	−80.392	−170.660	1232.16	−78.875	−170.653
1262.20	−76.770	−170.670	1211.63	−80.319	−170.644
1185.37	−82.187	−170.649	1242.39	−78.141	−170.642
1109.30	−87.588	−170.629	1208.37	−80.541	−170.634
1058.59	−91.202	−170.611	1187.84	−81.991	−170.628
1008.04	−94.832	−170.603	1228.86	−79.094	−170.638
957.72	−98.446	−170.580	1262.86	−76.704	−170.651
907.46	−102.065	−170.548		Run 14	
988.00	−96.265	−170.589	972.47	−97.371	−170.572
1038.50	−92.634	−170.598	1012.31	−94.515	−170.594
1139.70	−85.421	−170.632	1051.94	−91.676	−170.607
1190.19	−81.847	−170.651	1091.73	−88.832	−170.617
1241.24	−78.240	−170.660	1071.73	−90.259	−170.610
	Run 4		1111.66	−87.410	−170.620
1057.93	−91.260	−170.621	1151.78	−84.555	−170.628
1108.64	−87.645	−170.639	1101.52	−88.128	−170.613
1159.43	−84.032	−170.649	1081.59	−89.548	−170.606
1133.82	−85.848	−170.641	1141.58	−85.275	−170.621
1082.89	−89.470	−170.621	1121.46	−86.704	−170.614
1138.78	−85.500	−170.646		Run 15	
1210.24	−80.443	−170.669	972.39	−97.365	−170.560
1240.88	−78.278	−170.673	1012.06	−94.515	−170.576
1281.79	−75.391	−170.673	1051.80	−91.670	−170.591
1261.34	−76.830	−170.670	1091.58	−88.829	−170.603
	Run 6		1031.61	−93.116	−170.585
1058.76	−91.174	−170.594	991.84	−95.970	−170.571
1099.58	−88.274	−170.620	952.27	−98.818	−170.557
1140.33	−85.377	−170.634	912.64	−101.679	−170.540
1181.10	−82.484	−170.642	873.12	−104.532	−170.512
1160.57	−83.928	−170.627	902.90	−102.382	−170.533
1119.76	−86.824	−170.613	932.56	−100.236	−170.545
1079.03	−89.724	−170.599	982.00	−96.673	−170.563
1038.46	−92.632	−170.594	1021.74	−93.820	−170.579
1084.21	−89.341	−170.587	1061.50	−90.967	−170.591
1104.35	−87.919	−170.607	1111.45	−87.410	−170.605

[a] Listed in chronological order. Runs 2 and 15 used the "high-purity" {copper+copper(II) oxide} sample; runs 4, 6, and 14 used the "low-purity" {copper+copper(I) oxide} sample. Runs 2, 4, and 6 used the AD545L impedance buffer, whereas all other runs did not.

(equivalent to the assumption of a constant but non-zero value for $\Delta_f C^\circ_{p,m}$). The precision of the measurements, given by the scatter of the results around the regression, is ± 21 J·mol^{-1} (± 0.1 mV) (2s). This is the highest precision yet achieved in equilibrium measurements with zirconia solid electrolytes. The relative uncertainty is 0.025 per cent for $\Delta_f G^\circ_m(T)$, 0.25 per cent for $d\Delta_f G^\circ_m/dT$, and 10 per cent for $d^2\Delta_f G^\circ_m/dT^2$.

At this level or resolution, the curvature in $\Delta_f G^\circ_m(T)$ is clearly discernible. A strong

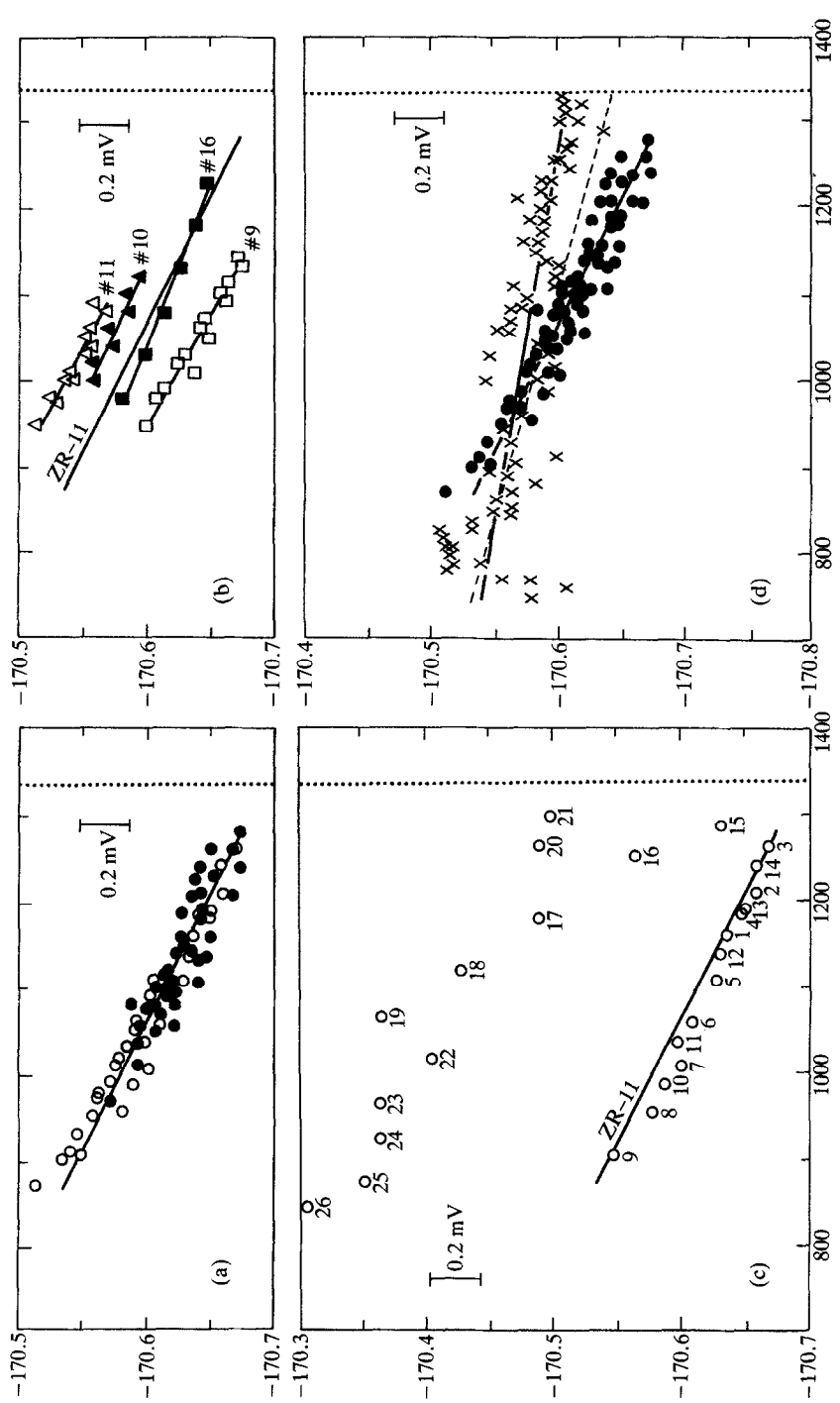

FIGURE 3. Third-law analysis ($p^\circ = 1 \times 10^5$ Pa). The vertical dotted line denotes the eutectic temperature at 1338 K. (a), Results for ZR-11 electrolytes. See text for discussion of the two different sample types. ●, {copper + copper(I) oxide} sample. ○, {copper + copper(II) oxide} sample. (b), Results for ZR-8Y and $SIRO_2$ electrolytes. Sample type was {copper + copper(I) oxide}. ■, ZR-8Y electrolyte, run 16. □, ZR-8Y electrolyte, run 9. ▲, $SIRO_2$ electrolyte, run 10. △, $SIRO_2$ electrolyte, run 11. (c), Oxidation of run 2. The numbers show the sequence in which the points were measured. (d), Comparison of our ZR-11 results with those reported by O'Neill.[2] ●, This study. ×, O'Neill (1988). The dashed line shows the trend obtained by combining the two sets.

test for the accuracy of the measurements can therefore be made by comparing the observed second derivative with the calorimetric values of $\Delta_f C^\circ_{p,m}$, since $d^2\Delta_f G^\circ_m/dT^2 = -\Delta_f C^\circ_{p,m}/T$. The average curvature, given by c in the 3-term regression, is $(6.0 \pm 0.5)\ J \cdot K^{-1} \cdot mol^{-1}$. This compares favorably with the JANAF[14] values for $\Delta_f C^\circ_{p,m}(T)$, which range from 6.1 to 7.3 $J \cdot K^{-1} \cdot mol^{-1}$ over this temperature interval. The absence of curvature or oscillations in the third-law trend (figure 3a) is another indicator of good agreement between the observed second derivative and the calorimetric values for $\Delta_f C^\circ_{p,m}$.

The difference between $d\Delta_f G^\circ_m/dT = -\Delta_f S^\circ_m$ and the calorimetric entropy is given by the slope of the third-law trend. The observed slope of $-(0.35 \pm 0.27)$ $J \cdot K^{-1} \cdot mol^{-1}$ is smaller than the statistical uncertainty in the JANAF value of $\Delta_f S^\circ_m(T)$ at these temperatures ($\pm 0.35\ J \cdot K^{-1} \cdot mol^{-1}$ at 298.15 K). This indicates that the observed first derivative is in very good agreement with the calorimetric value of $\Delta_f S^\circ_m$.

The average value for the standard molar enthalpy of formation, $\Delta_f H^\circ_m(298.15\ K)$, calculated from the third-law analysis of the ZR-11 results is $-(170.61 \pm 0.07)\ kJ \cdot mol^{-1}$ ($n = 69$). This is in excellent agreement with the combustion-calorimetric value of $-(170.8 \pm 1.3)\ kJ \cdot mol^{-1}$ reported by Mah *et al.*[15]

Tables 2 and 3 give the results obtained with the ZR-8Y and $SIRO_2$ electrolytes. The third-law analysis of these measurements is shown in figure 3(b). All four runs used the "low-purity" {copper + copper(I) oxide} sample.

For the ZR-8Y electrolytes, the results from run 16 are in near perfect agreement with the ZR-11 trend, but the results from run 9 are about $40\ J \cdot mol^{-1}$ more negative. Run 9 was trouble-free and there is no obvious explanation for this anomaly. This is the only experiment that gave any indication of values more negative than the ZR-11 trend. The slope of run 16 appears to have been affected by barely perceptible oxidation at higher temperatures.

For the $SIRO_2$ electrolytes, the results are 20 to $40\ J \cdot mol^{-1}$ more positive than the ZR-11 trend. Two factors that might explain this minor difference are the uncertainty in extrapolating the $SIRO_2$ residual (± 0.2 mV) and the possibility of an undetected vacuum leak ($< 10^{-6}\ Pa \cdot m^3 \cdot s^{-1}$). Except for the one electrolyte actually used in these two runs, all of the $SIRO_2$ electrolyte tubes that we tested had obvious vacuum leaks. Other measurements in our laboratory have shown that even the smallest detectable vacuum leak can cause measurable oxidation.

The total scatter around the ZR-11 trend for both the ZR-8Y and $SIRO_2$ electrolytes is only $\pm 40\ J \cdot mol^{-1}$. Compared with previous e.m.f. studies,[16,17] this is the best agreement yet achieved between solid electrolytes of different composition.

Our experiments typically showed measurable oxidation of the sample after 2 to 3 d at high temperature. In cells with a large difference in $p(O_2)$ between the sample and the reference, this is a common phenomenon that is usually attributed to electronic conduction within the zirconia electrolyte.[2,18-21] The present observations are noteworthy only because the initial oxidation errors are significantly smaller than the 1 to 2 mV resolution typical of previous e.m.f. studies. Figure 3(c) shows the typical pattern of oxidation. The initial effect was only about 0.1 mV, and the error did not exceed 1.0 mV until 32 h after the beginning of

TABLE 2. Experimental results for the cell Pt|(Cu+Cu_2O)|ZR-8Y|O_2 ($p^\circ = 1 \times 10^5$ Pa)|Pt [a]

T/K	$\Delta_f G^\circ_m(T)$/kJ·mol^{-1}	$\Delta_f H^\circ_m$(298.15 K)/kJ·mol^{-1}	T/K	$\Delta_f G^\circ_m(T)$/kJ·mol^{-1}	$\Delta_f H^\circ_m$(298.15 K)/kJ·mol^{-1}
	Run 9		1019.94	−93.998	−170.626
1008.56	−94.830	−170.639	1060.75	−91.080	−170.644
1050.16	−91.847	−170.650	1101.70	−88.161	−170.659
1091.46	−88.899	−170.664	1142.76	−85.243	−170.673
1132.44	−85.982	−170.676		Run 16	
1111.98	−87.433	−170.666	979.23	−96.891	−170.581
1070.90	−90.356	−170.648	1028.91	−93.326	−170.600
1030.04	−93.276	−170.632	1078.49	−89.779	−170.615
989.22	−96.203	−170.615	1128.31	−86.228	−170.627
948.66	−99.124	−170.601	1178.41	−82.672	−170.639
979.15	−96.923	−170.608	1228.77	−79.111	−170.649

[a] Listed in chronological order.

oxidation (point 26). In e.m.f. measurements with lower resolution, the loss of sample equilibrium indicated by such deviations could easily be overlooked. (Tables 1, 2, and 3 include only results that were collected before the onset of oxidation.)

4. Comparison with previous studies

The e.m.f. measurements of O'Neill[2] are noteworthy because he has also made significant progress towards overcoming the problems with thermal residuals that limited the accuracy of our earlier joint work.[1] However, his method of correcting for the residuals is quite different from that reported here, and his results are completely independent of ours.

Figure 3(d) compares our ZR-11 results with those reported in table 1 of O'Neill.[2]

TABLE 3. Experimental results for the cell Pt|(Cu+Cu_2O)|$SIRO_2$|O_2 ($p^\circ = 1 \times 10^5$ Pa)|Pt [a]

T/K	$\Delta_f G^\circ_m(T)$/kJ·mol^{-1}	$\Delta_f H^\circ_m$(298.15 K)/kJ·mol^{-1}	T/K	$\Delta_f G^\circ_m(T)$/kJ·mol^{-1}	$\Delta_f H^\circ_m$(298.15 K)/kJ·mol^{-1}
	Run 10		1039.28	−92.537	−170.558
999.15	−95.431	−170.560	999.36	−95.400	−170.544
1039.19	−92.561	−170.575	1029.36	−93.247	−170.554
1079.17	−89.703	−170.587	1059.34	−91.096	−170.559
1119.23	−86.845	−170.596	1089.35	−88.946	−170.560
1099.04	−88.279	−170.587	1049.23	−91.819	−170.555
1059.05	−91.129	−170.571	1009.30	−94.680	−170.542
1019.11	−93.990	−170.559	979.38	−96.826	−170.527
			949.71	−98.960	−170.513
	Run 11		974.55	−97.178	−170.530
1079.20	−89.682	−170.569	999.40	−95.391	−170.539

[a] Listed in chronological order.

There is extensive overlap in the measured values of $\Delta_f G^\circ_m(T)$, especially at lower temperatures. O'Neill's results are less precise than ours ($\pm 40\ J \cdot mol^{-1}$, compared with $\pm 21\ J \cdot mol^{-1}$), but give a somewhat smaller third-law slope ($-0.12\ J \cdot K^{-1} \cdot mol^{-1}$, compared with $-0.35\ J \cdot K^{-1} \cdot mol^{-1}$). The average value of $\Delta_f H^\circ_m(298.15\ K)$ from O'Neill's results is $-(170.57 \pm 0.06)\ kJ \cdot mol^{-1}$ ($n = 71$).

The results of these two studies are essentially identical, and in our opinion there is no clear reason to prefer one over the other. Both sets of results are fully consistent with one another and with the JANAF values of $\Delta_f C^\circ_{p,m}$, $\Delta_f S^\circ_m$, and $\Delta_f H^\circ_m$. We have therefore combined the two sets in order to calculate the dashed line in figure 3(d). The slope of the dashed line is $-(0.19 \pm 29)\ J \cdot K^{-1} \cdot mol^{-1}$ and the scatter is $\pm 51\ J \cdot mol^{-1}$. The average value of $\Delta_f H^\circ_m(298.15\ K)$ for the combined set is $-(170.59 \pm 0.08)\ kJ \cdot mol^{-1}$ ($n = 140$).

This is our recommended value for the $\Delta_f H^\circ_m(Cu_2O)$. It is well within the error limits of the combustion-calorimetric value of $-(170.8 \pm 1.3)\ kJ \cdot mol^{-1}$ measured by Mah *et al.*[15] and later accepted by the critical review of Santander and Kubaschewski.[22] It is also within the uncertainty of the value of $-(170.71 \pm 2.1)\ kJ \cdot mol^{-1}$ adopted by JANAF.[14] See figure 6 of reference 1 for a comparison with several older less accurate e.m.f. studies.

In our previous study,[1] we obtained a value of $-(170.51 \pm 0.2)\ kJ \cdot mol^{-1}$ for $\Delta_f H^\circ_m(298.15\ K)$. However, this value did not take into account the humidity of the air reference gas. Using 800 Pa as a typical value of $p(H_2O)$ for Canberra,[2] we can calculate an approximate correction of $-45\ J \cdot mol^{-1}$ to the value of $\Delta_f G^\circ_m(1300\ K)$. This gives a humidity-corrected value of $-(170.55 \pm 0.2)\ kJ \cdot mol^{-1}$ for $\Delta_f H^\circ_m(298.15\ K)$, in excellent agreement with the recommended value derived above.

We now have three independent e.m.f. studies which give values of $\Delta_f H^\circ_m(Cu_2O, 298.15\ K)$ that span a range of only $60\ J \cdot mol^{-1}$! The *only* factor common to all three studies is the use of CaO-doped slip-cast electrolytes from the same manufacturer (ZR-11 and ZR-15). However, our new measurements with the ZR-8Y and $SIRO_2$ electrolytes confirm the ZR-11 results to within $\pm 40\ J \cdot mol^{-1}$. The accuracy of our recommended value for $\Delta_f H^\circ_m(298.15\ K)$ therefore appears to be limited only by random errors.

Using our recommended value of $\Delta_f H^\circ_m(298.15\ K)$ together with the JANAF standard molar entropy and heat-capacity values, we can *calculate* the recommended value of $\Delta_f G^\circ_m(Cu_2O)$ at any temperature. The 3-term regression of the (noise-free) calculated values from 700 to 1338 K gives

$$\Delta_f G^\circ_m(T)/(J \cdot mol^{-1}) \pm 5 = -174043 + 123.541(T/K) - 6.500(T/K)\ln(T/K).$$

This work was supported by NSF grant EAR-8417131 to R. J. Arculus. We would like to thank Susan Fast for preparing the diagrams, Scott Baird for assistance with electronics, and Bill Wilcox for supervising the construction of our new laboratory.

REFERENCES

1. Holmes, R. D.; O'Neill, H. St. C.; Arculus, R. J. *Geochim. Cosmochim. Acta* **1986,** 50, 2439.
2. O'Neill, H. St. C. *Am. Mineral.* **1988,** 73, 470.

3. Quinn, T. J. *Temperature*. Academic Press: New York. **1983,** pp. 128–132.
4. Tretyakov, J. D.; Muan, A. *J. Electrochem. Soc.* **1969,** 116, 331.
5. Sreedharan, O. M.; Chandrasekharaiah, M. S.; Karkhanavala, M. D. *High Temp. Sci.* **1977,** 9, 109.
6. Emmett, P. H.; Shultz, J. F. *J. Am. Chem. Soc.* **1933,** 55, 1376.
7. Powell, R. L.; Hall, W. J.; Hyinck, C. H., Jr.; Sparks, L. L.; Burns, G. W.; Scroger, M. G.; Plumb, H. H. *U.S. Natl. Bur. Stand. Monogr.* **1974,** 125.
8. CIPM [Comité International des Poids et Mesures] *Metrologia* **1975,** 12, 7.
9. Coates, P. B.; Andrews, J. W. *J. Phys. F: Metal Phys.* **1978,** 8, 277.
10. Jones, T. P.; Tapping, J. *Temperature: Its Measurement and Control in Science and Industry*. Vol. 5. Schooley, J. F.: editor. AIP Publ.: New York. **1982,** p. 169.
11. Riddle, J. L.; Furukawa, G. T.; Plumb, H. H. *U.S. Natl. Bur. Stand. Monogr.* **1973,** 126.
12. Bentley, R. E.; Jones, T. P. *High Temp.-High Pressures* **1980,** 12, 33.
13. Cohen, E. R.; Taylor, B. N. *U.S. Natl. Bur. Stand. J. Res.* **1987,** 92, 85.
14. Chase, M. W., Jr.; Davies, C. A.; Downey, J. R., Jr.; Frurip, D. J.; McDonald, R. A.; Syverud, A. N. *J. Phys. Chem. Ref. Data* **1985,** 14, Suppl. 1.
15. Mah, A. D.; Pankratz, L. B.; Weller, W. W.; King, E. G. *U.S. Bur. Mines Rept. Invest. 7026.* **1967.**
16. Moriyama, J.; Sato, N.; Asao, H. *Mem. Fac. Eng., Kyoto Univ.* **1969,** 31, 253.
17. Kiukkola, K.; Wagner, C. *J. Electrochem. Soc.* **1957,** 104, 379.
18. Giddings, R. A.; Gordon, R. S. *J. Am. Ceram. Soc.* **1973,** 56, 111.
19. Ramanarayanan, T. A. *Solid Electrolytes and their Applications*. Subbarao, E. C.: editor. Plenum: New York. **1980,** p. 81.
20. O'Neill, H. St. C. *Am. Mineral.* **1987,** 72, 67.
21. O'Neill, H. St. C. *Am. Mineral.* **1987,** 72, 280.
22. Santander, K. H.; Kubaschewski, O. *High Temp.-High Pressures* **1975,** 7, 573.